COMPARATIVE VISUALIZATION FOR TWO-DIMENSIONAL GAS CHROMATOGRAPHY

by

Ben Hollingsworth

A THESIS

Presented to the Faculty of

The Graduate College at the University of Nebraska

In Partial Fulfillment of Requirements

For the Degree of Master of Science

Major: Computer Science

Under the Supervision of Professor Stephen E. Reichenbach

Lincoln, Nebraska

December, 2004

COMPARATIVE VISUALIZATION FOR TWO-DIMENSIONAL GAS CHROMATOGRAPHY

Ben Hollingsworth, M.S.

University of Nebraska, 2004

Advisor: Stephen E. Reichenbach

This work investigates methods for comparing two datasets from comprehensive two-dimensional gas chromatography (GC×GC). Because GC×GC introduces inconsistencies in feature locations and pixel magnitudes from one dataset to the next, several techniques have been developed for registering two datasets to each other and normalizing their pixel values prior to the comparison process. Several new methods of image comparison improve upon pre-existing generic methods by taking advantage of the image characteristics specific to GC×GC data. A newly developed colorization scheme for difference images increases the amount of information that can be presented in the image, and a new "fuzzy difference" algorithm highlights the interesting differences between two scalar rasters while compensating for slight misalignment between features common to both images.

In addition to comparison methods based on two-dimensional images, an interactive three-dimensional viewing environment allows analysts to visualize data using multiple comparison methods simultaneously. Also, high-level features extracted from the images may be compared in a tabular format, side by side with graphical representations overlaid on the image-based comparison methods. These image processing techniques and high-level features significantly improve an analyst's ability to detect similarities and differences between two datasets.

ACKNOWLEDGEMENTS

I thank Dr. Steve Reichenbach for his guidance and insight throughout this research. Dr. Mingtian Ni and Arvind Visvanathan also provided invaluable assistance in understanding the GC×GC process and integrating the implementation of this research into the GC Image software package. I also thank Capt. Rick Gaines of the United States Coast Guard Academy, a "real world" GC×GC analyst, for his input regarding this research.

Contents

List of Figures

List of Tables

Chapter 1

Introduction

The history of two-dimensional gas chromatography dates back to the 1960's.[3] With the introduction of comprehensive two-dimensional gas chromatography (GC$\times$GC) in the early-1990's,[11] the ability to separate large numbers of chemicals took a huge leap forward, and the use of this technology for real-world applications has grown quickly. As GC$\times$GC datasets have grown both more complex and more heavily used, the need to analyze these datasets and compare the results of multiple datasets has become more apparent.[20] In fact, Mondello *et al.* suggested in 2002 that the lack of good analysis software was perhaps the most significant obstacle to overcome in order for GC$\times$GC to become more widely accepted.[12]

The data generated by GC$\times$GC is typically represented as a two-dimensional image of scalar values. Therefore, generic image processing techniques for change detection may be applied as elementary first steps toward detection of similarities and differences between two datasets. Several of these techniques are described in Section 1.2. However, post-processing of individual images with software such as GC Image[16] can extract a large amount of information about the dataset from the image and store it as metadata along with the image data. By making use of this metadata and by modifying generic image processing techniques to work better with the specific types of images produced by GC×GC, an analyst's ability to detect similarities and differences between two datasets can be significantly improved.

1.1 Dataset Details

Comprehensive two-dimensional gas chromatography is a recent extension of the well-established field of one-dimensional gas chromatography. Compared with the one-dimensional form, GC×GC increases the peak separation capacity by an order of magnitude and can readily distinguish several thousand unique chemical compounds.[2]

GC×GC is performed by taking one GC column and appending to it a second GC column having retention characteristics which are significantly different than those of the first column. The two columns are joined by a modulator which traps the chemicals as they are eluted from the first column and periodically injects them into the second column. A detector is placed at the end of the second column to measure and periodically report the concentration and/or other measures of chemicals being eluted.[12] A diagram of the basic hardware configuration is shown in Figure 1.1. While the first column typically takes many minutes or hours to process the entire chemical sample, the second column usually requires only a few seconds. Ideally, the modulator between the columns is timed so that the entire effluent exits the second column before the next batch is released into it.[2] A detector running at a typical sampling frequency of 100 Hz is able to make several hundred distinct measurements for each pass through the second column, and there are usually several hundred such passes required before all chemicals are eluted from the first column.

The raw data collected by a flame-ionization detector (FID) is multiplied by a constant gain coefficient to produce a one-dimensional stream of floating point values

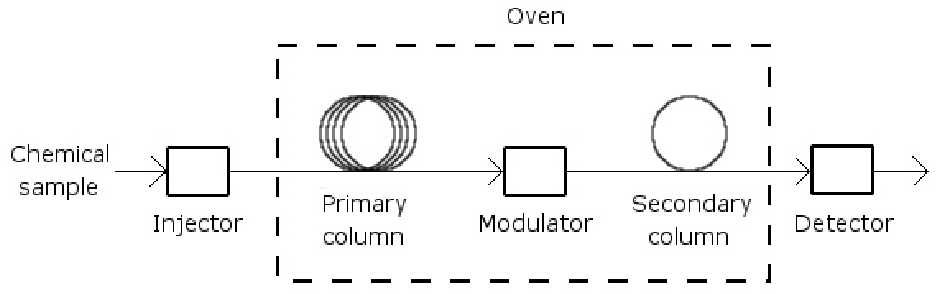

Figure 1.1: Typical GC×GC hardware configuration

indicating the concentration of chemicals detected during each interval while exiting the second column. To transform the data into a two-dimensional image, the raw data stream is divided into sections, with each section representing the data collected during one pass through the second column. The sections are stacked together, one per row, to form a two-dimensional image. This procedure is demonstrated in Figure 1.2. The dimensions of the resulting image can be measured either in pixels (the number of measurement intervals of the detector) or in the time required for the given pixel to elute from each GC column.[8]

The resulting GC×GC FID images vary greatly in size depending on the equipment parameters of each run, ranging from fewer than 50x500 pixels to more than 1000x5000 pixels. These images contain achromatic intensities, which allows the use of any desired color scheme in order to assist in visualization. Prior to further automated analysis of these images, basic post-processing generally is performed on these images to perform baseline flattening and remove undesirable artifacts such as the solvent front.[20] Portions of a sample dataset are shown in Figure 1.3.

The GC×GC image data is comprised primarily of a large background area with small pixel values. Scattered throughout the image are small clusters of pixels with larger values, known as *blobs*, which represent higher concentrations of chemicals emerging from the GC×GC equipment at a particular time. In each blob, the pixel

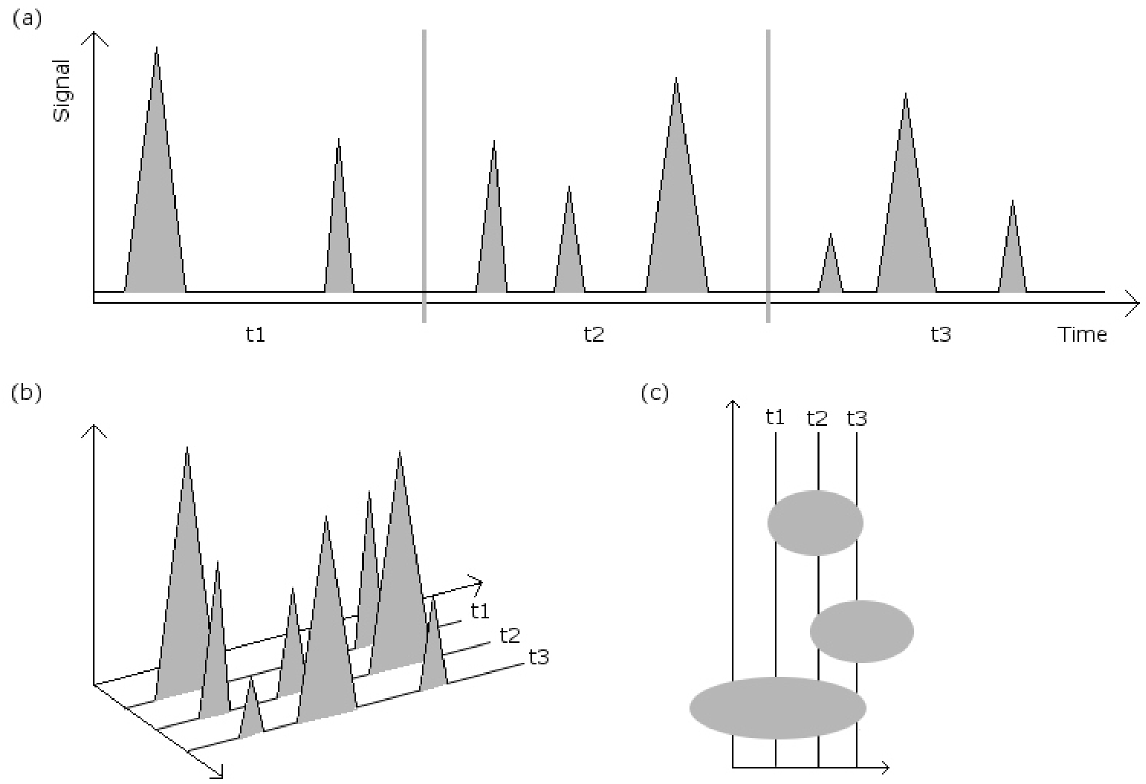

Figure 1.2: The GC×GC data collection process. The linear output data (a) is received from the detector and split into sections representing individual passes through the second column. Those sections are stacked together (b) and treated as a 2D image of peaks (c).

which has the largest value is known as the *peak*. These blobs are the primary features of interest in the datasets, as they indicate which chemicals were found in the input sample. One important feature of any GC analysis software is the ability for a user (either manually or automatically) to identify the chemicals represented by various blobs in an image and store additional metadata information about those blobs, including a unique compound name and various statistics for each blob. Once created, this metadata can be used for many purposes, including increasing the accuracy of the comparative visualization tools.

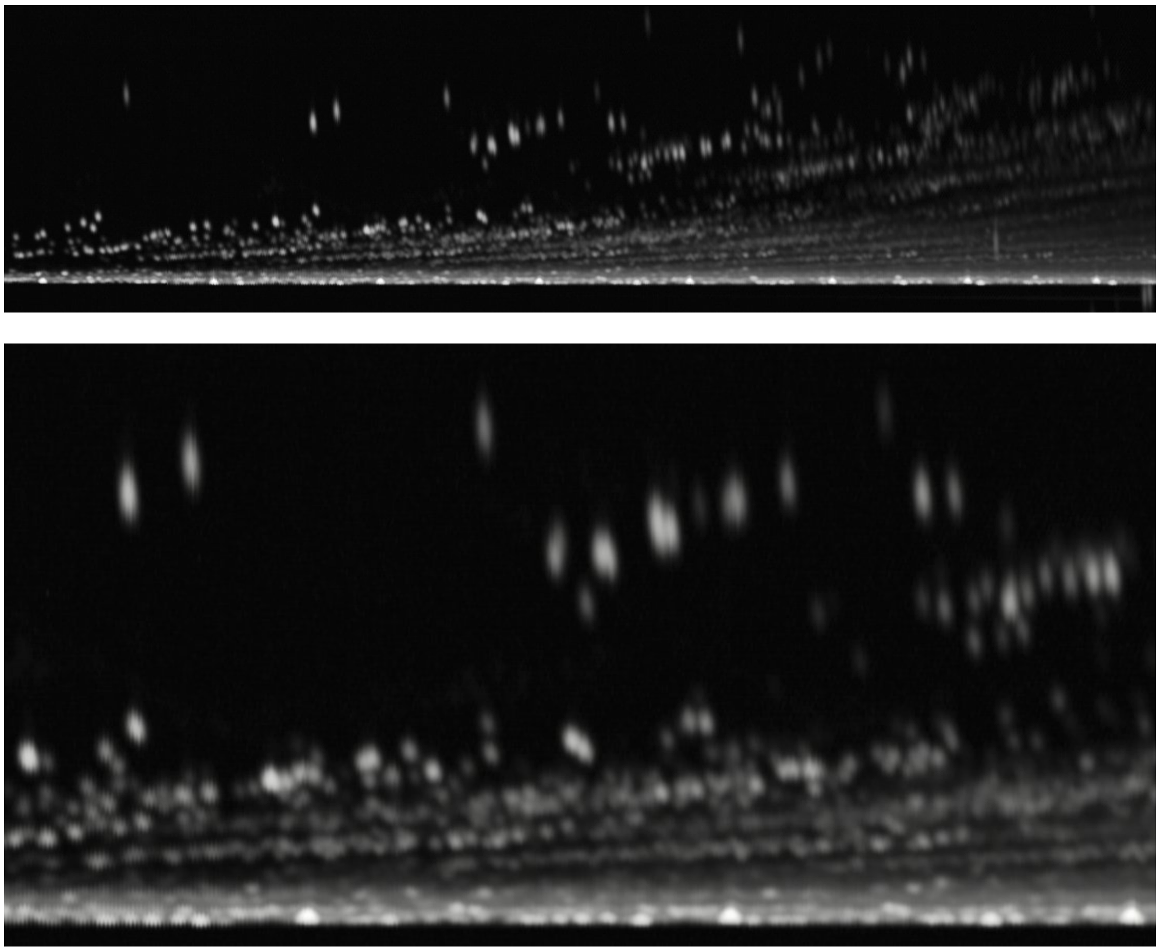

Figure 1.3: Sample GC×GC data: full image (top) and enlarged subsection (bottom)

1.2 Previous Work

Because the detection of changes in the GC×GC data deals primarily with analyzing the image data, traditional generic image comparison techniques are applicable.

The side-by-side comparison of two images is the oldest method of image comparison, predating the use of computers. The biggest problem with this method is that it requires the user to visually determine the differences between the two images. Small, but potentially significant, differences in location and intensity are overlooked easily.

With the advent of digital images and graphical computer displays, one of the earliest methods employed was to subtract the individual pixel values of one image from the corresponding pixel values in the other image in order to form a *difference image* (or *subtraction image*) that contains only the differences between them.[7] Kunzel modified this technique by using the difference image to determine the hue of the image, while the intensity was determined by the pixel value of one of the original images.[9]

The three-band nature of RGB color images lends itself to another simple comparison technique known as an *addition image*, where two or three greyscale images are combined to produce a color image. One image is used as the red band, another is used as the green band, and another (if desired) is used to form the blue band. The intensity of each pixel in the output image will be similar to that of the largest input value. The hue of each pixel will be determined by the combination of the three input pixel values in the RGB color space.[19]

Another method of image comparison is to use a *flicker image*, where two images are alternately displayed in the same location on the screen and the user can rapidly switch between them.[10] Although the identification of differences is still left to the user, the fact that both images occupy the same display space makes these differences much more obvious.

Although these basic techniques work reasonably well for detecting changes in generic images, the use of blob metadata and other image characteristics specific to GC$\times$GC allows for improvement in comparison accuracy and ease of analysis.

Chapter 2

Dataset Preprocessing

Most GC×GC analysis tasks operate on a single dataset. When comparing two images, the dataset currently selected for analysis is known as the *analyzed image*. Within the image comparison process, a second image is selected for comparison against the primary (analyzed) image. This second image is termed the *reference image*.

Before any comparison can be performed, the data in the reference image must be transformed so that corresponding features in the two images occupy the same pixel location. The magnitude of the pixel values in the reference image must also be scaled so that pixels representing identical physical characteristics will have the same pixel value in the two images. These two steps are critical to the software's ability to deemphasize common features and emphasize only the real differences.

2.1 Data Transformation

Due to the nature of the GC×GC process, two samples of the same mixture produce datasets that have peaks which are in slightly different locations (indicating that they were eluted at slightly different times) and which have slightly different

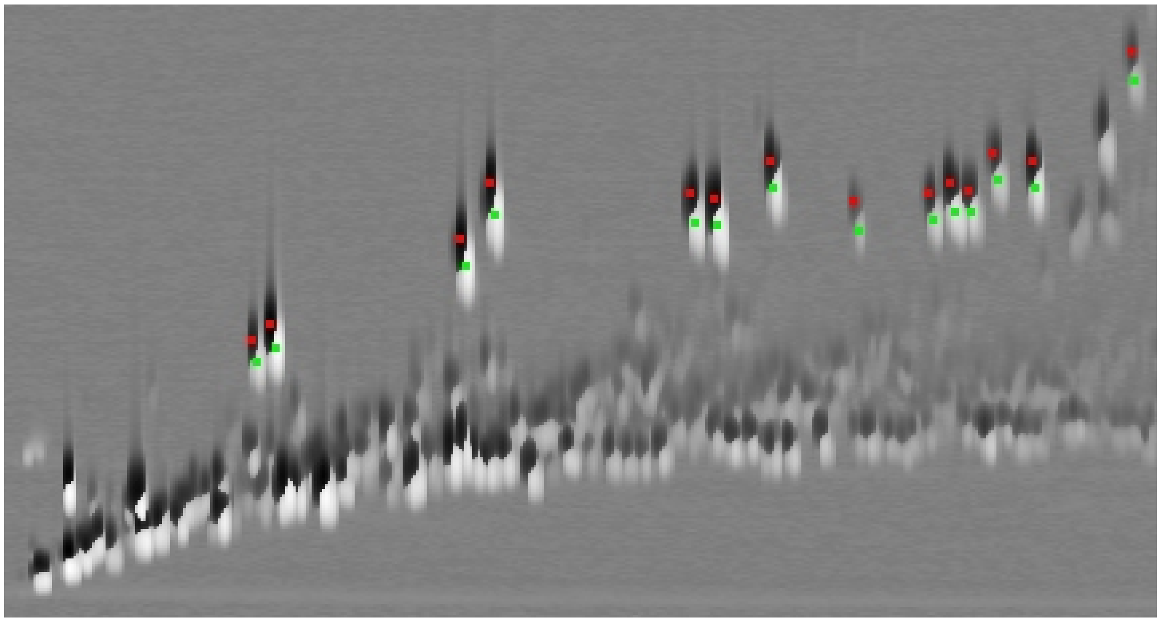

Figure 2.1: Example difference image showing blob locations before image registration. Red dots indicate reference peaks. Green dots indicate analyzed peaks.

magnitudes. This occurs as a result of small fluctuations in the operating parameters of the GC×GC equipment, such as temperature variations or slight differences in the time and amount of injection.[20] This is demonstrated in Figure 2.1, which shows a difference image for two un-registered datasets. Therefore, prior to comparing two output datasets, the two images must be registered so that the peaks common to both images are located as close as possible to the same pixel locations in both images. This requires that one or both of the two images be rotated, translated, scaled, and/or sheared using a two-dimensional affine transformation.[13] The reference image is then convolved using bilinear interpolation so that the resulting pixel values and locations match those of the analyzed image as accurately as possible.[17]

Although either or both of the images could theoretically be transformed in order bring the two images into alignment, the decision was made to transform only the reference image. This was done primarily because our implementation of these comparative visualization techniques is part of a larger software package for analysis of GC×GC data.[16] The analyzed image is the one that has previously been selected for analysis (hence the name). The reference image is selected only for comparison within this part of the application. Keeping the analyzed image in its original orientation provides a more intuitive environment for the analyst using this software, because the user is most likely already familiar with the image in that form.

To determine the transformation that maps the reference image onto the analyzed image, a least-squares fit algorithm is run on the peak locations of a subset of the blobs that exist in both images. The selection of this subset is discussed below. The peak location of each blob is determined by GC×GC analysis software prior to the comparison process and stored as metadata along with the GC×GC image data. The blobs are matched between the two images based on the compound name (if any) assigned to each blob. First, unnamed blobs are eliminated from consideration. Next, blobs which share the same name with another blob in the same dataset are eliminated from consideration. Such blobs occur infrequently, and usually as a result of operator error when assigning the names. Finally, for each remaining blob in the analyzed image, an exhaustive search is performed within the remaining blobs from the reference image for a blob with the same name. If one is found, that pair of blobs is added to a list of blobs to be used in the least-squares fit. The least-squares fit algorithm determines the optimal transform which, when applied to the pixel coordinates of each peak from the reference image, minimizes the sum of the squared Euclidean distances between the coordinates of each reference peak and the coordinates of the corresponding analyzed peak.[4] The squared error sum E is computed as

$$E = \sum_{b \in blob\ list} (x_{a_b} - x_{r_b})^2 + (y_{a_b} - y_{r_b})^2$$

where a_b and r_b are the corresponding analyzed and reference peaks for blob b, and

x and y are the pixel coordinates for the specified peak.

Frequently, there will be several blobs in the datasets that, although identified as the same compound, will be located in significantly different positions even after the reference image has been transformed. Pairs of peaks that are excessively mis-matched between the two images tend to reduce the accuracy of the transformation. To compensate for this, two different approaches were developed.

In the first approach, a two-stage algorithm is used when computing the least-squares fit. After the first transform is computed from all shared peaks, the peak locations from the reference image are transformed, and the Euclidean distance is computed between the analyzed image peaks and the transformed corresponding reference image peaks. Those peaks whose distances are in the largest 25% are removed from consideration (while ensuring that at least three peaks are retained), and the least-squares fit is recomputed on the remaining peaks to obtain the final affine transformation. This simple modification to the basic algorithm assumes that no more than 25% of the blobs will be grossly mis-aligned and that the remaining 75% are sufficient to produce a good transformation. This has proven to work well in practice. The results of this elimination process are demonstrated in Figure 2.2.

A second, iterative approach to pruning excessively mismatched peaks also was developed. At each iteration, a least-squares fit is first computed using the current list of peaks common to both images. The peak locations from the reference image are then transformed, and the Euclidean distance is computed between each analyzed peak and the corresponding transformed reference peak. The peak with the largest distance is then compared to a predetermined threshold value. If the distance is above the threshold, that peak is removed from the list and the process is repeated using the remaining peaks. If the distance is below the threshold, then the loop terminates and the last transform is used for the rest of the comparative visualization process.

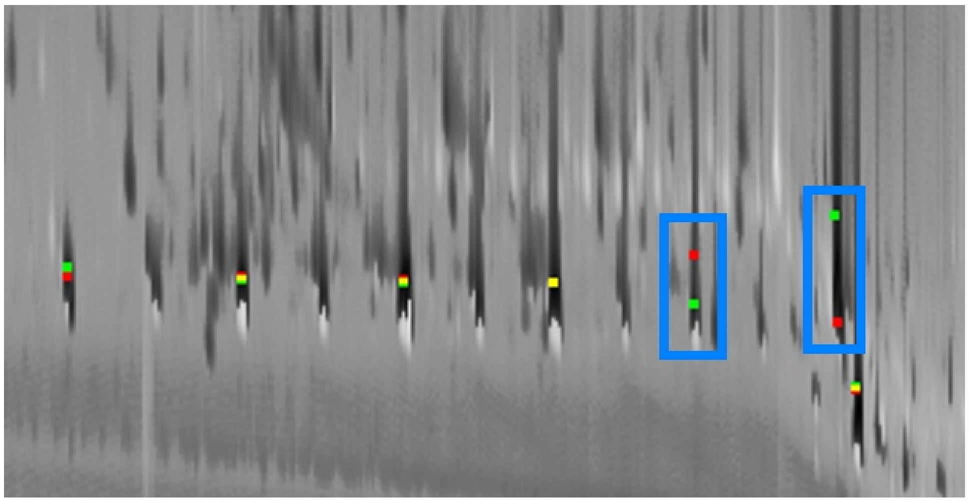

Figure 2.2: Example difference image showing peak locations after image registration. Red dots indicate reference peaks. Green dots indicate analyzed peaks. Yellow indicates overlapping dots. The two peak pairs marked in blue are excessively misaligned (by 16 pixels on the left and 35 pixels on the right), and were therefore removed from consideration when computing the registration transform.

This loop will automatically terminate when no more than three peaks remain as long as a non-zero threshold is used, because a least-squares fit on three points will always produce a perfect match (within the limits of floating point arithmetic).

The advantage of this algorithm is its ability to more accurately determine exactly which blobs are excessively misaligned and therefore should be ignored when computing the least-squares fit. The disadvantage is that the performance of the algorithm relies heavily on the choice of an appropriate threshold value—something that can be difficult to determine. Using a threshold that is too large will include too many misaligned peaks and not solve the problem for which the algorithm was created. Using a threshold that is too small may work well for some images, but throw out the majority of the peaks from others.

Experimentation with this algorithm was done on nine different pairs of images having 14–18 blobs common to each pair. The algorithm was run on each pair using thresholds varying from 3 to 20 pixels. For each threshold, the mean squared error (MSE) was computed for each of the image pairs. The MSE is defined as

$$MSE = \frac{1}{N} \sum_{all\ pixels} (v_a - v_r)^2$$

where N is the number of pixels in each image, v_a is the pixel value from the analyzed image, and v_r is the corresponding pixel value from the reference image.[1]

The threshold which produced the smallest MSE varied greatly (from 3 to 20 pixels) even within this small test set, although a threshold of 5 most frequently produced the best results. The results of these tests are presented in Table 2.1 on page 13. The MSE also was computed by applying the aforementioned "drop 25%" algorithm to each of the image pairs. The "drop 25%" MSE was sometimes much smaller than, sometimes much larger than, and sometimes comparable to the best MSE produced by the iterative algorithm. Regardless of the threshold used, neither of the algorithms performed consistently better or worse than the other. Optimal performance of the iterative algorithm relies on choosing the appropriate threshold, and this threshold appears to vary widely even among similar datasets. This makes the algorithm difficult to use effectively. Because of this, the iterative algorithm was set aside pending further research, and the "drop 25%" algorithm was chosen for use in this application.

Once an acceptable transform has been generated, the reference image and all associated blob metadata is transformed, and a new working copy of the reference image is created that contains only those pixels whose new locations fall inside the bounds of the analyzed image. This working image is the same size as the analyzed image. Those pixels in the new working copy which were beyond the bounds of the original, unmodified reference image are masked out and do not affect further

Selection Algorithm	MSE for each image pair			
	G1P1	G1P2	G1P3	G1P4
Drop 25%	38.238	81.462	131.129	142.430
Peaks Retained	13/18	13/18	13/18	13/18
Threshold 3	28.780	56.141	93.663	49.527
Peaks Retained	17/18	16/18	15/18	15/18
Threshold 5	28.780	56.421	56.269	33.907
Peaks Retained	17/18	17/18	17/18	17/18

Selection Algorithm	MSE for each image pair				
	G2P1	G2P2	G2P3	G2P4	G2P5
Drop 25%	1678083	2714662	1600533	3832121	2068510
Peaks Retained	10/14	10/14	10/14	10/14	10/14
Threshold 3	968255	3192925	3533956	3288412	1991317
Peaks Retained	7/14	8/14	5/14	5/14	6/14
Threshold 5	1115525	3065092	3083609	3288412	2076938
Peaks Retained	10/14	9/14	7/14	5/14	8/14
Threshold 7	1115525	3212437	3145972	4726396	2068510
Peaks Retained	10/14	10/14	8/14	8/14	10/14
Threshold 10	1115525	3564295	3155536	4659423	2068510
Peaks Retained	10/14	12/14	9/14	9/14	10/14
Threshold 15	1684530	3564295	3241191	4593703	2437782
Peaks Retained	11/14	12/14	10/14	10/14	11/14
Threshold 20	1685073	3564295	2650232	4417996	2600084
Peaks Retained	12/14	12/14	13/14	11/14	12/14

Table 2.1: MSE and number of peaks retained for both blob selection algorithms on two groups of image pairs. The images within each group were created from different runs on the same chemical sample and were therefore very similar. For the first group, thresholds from 5–20 yielded identical results.

processing. These pixels are displayed as grey blocks at the top and bottom of the reference image in Figure 2.3 on page 14. From this point forward in the image comparison process, all mentions of the reference image refer to this transformed working copy, not to the original reference image.

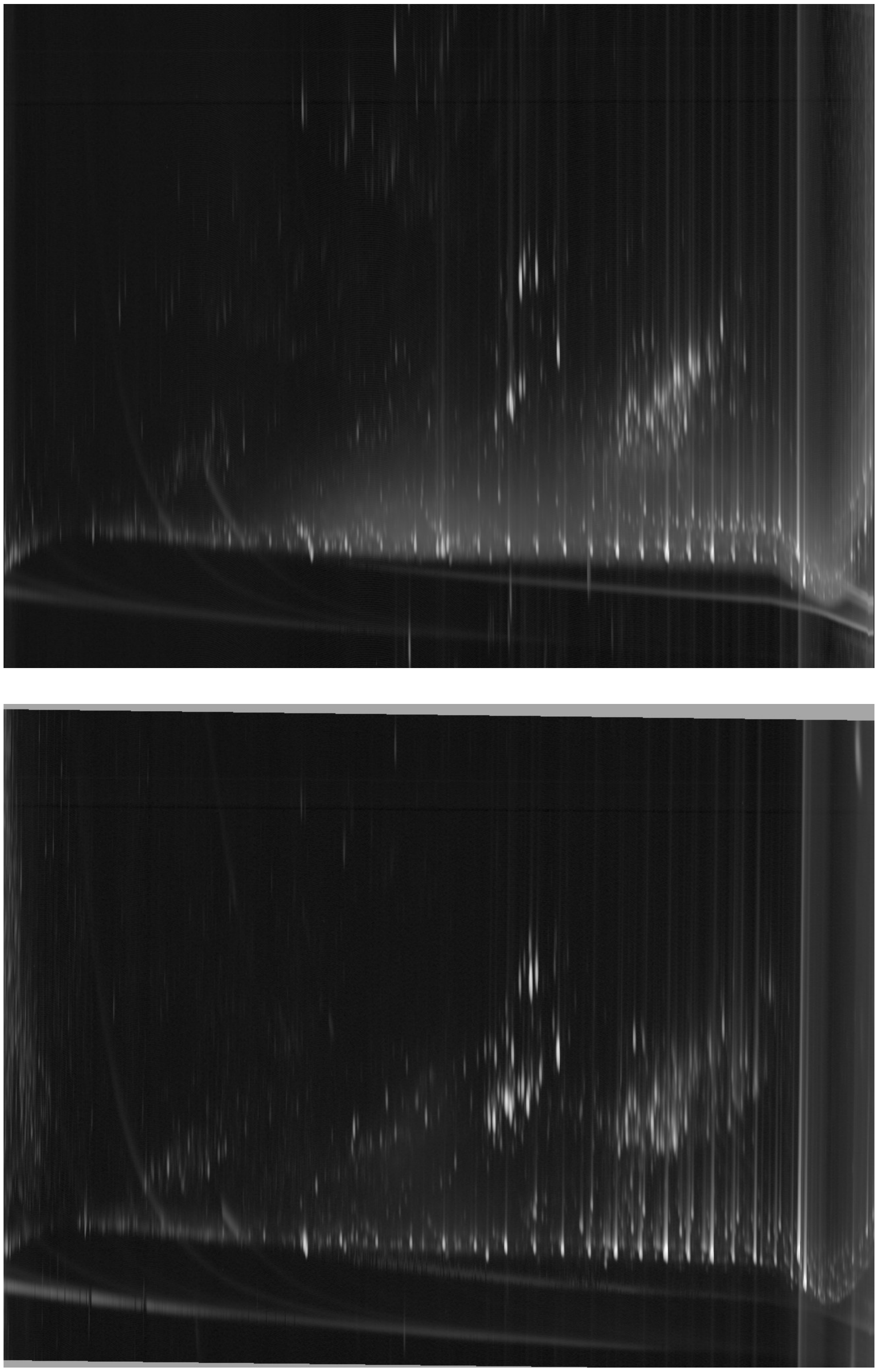
Figure 2.3: Analyzed image (top) and transformed reference image (bottom)

2.2 Data Normalization

Due to the nature of GC×GC, even when two tests are performed on two identical samples, the concentrations of each compound appearing in the output data will differ somewhat. These differences in pixel values, if left unaltered, would incorrectly indicate differences in the amount of each compound when no difference actually existed. To avoid this problem, the reference image is normalized by applying a linear scale factor to every pixel value as well as to the relevant features in the blob metadata (such as the pre-computed volume of each blob). This makes most corresponding pixel values approximately equal between the two images and makes differences in peak height more apparent.

This normalization factor is computed using a subset of the blobs which are common to both the analyzed and the reference image. The volume V_b of blob b is defined as the sum of the values v_p for all pixels p contained in the blob.

$$V_b = \sum_{p \in b} v_p$$

The normalization scale factor S is then defined as the sum of the blob volumes from the analyzed image divided by the sum of the blob volumes from the reference image.

$$S = \frac{\sum_{b \in analyzed} V_b}{\sum_{b \in reference} V_b}$$

Finally, the value v_p of each pixel p in the reference image is multiplied by the scale factor.

$$v'_p = v_p \times S,\ \forall p \in \mathit{reference\ image}$$

The collection of blobs used for the normalization process is determined using one of three methods. If there are any *internal standard* blobs defined in the two images, those blobs are used for normalization. An internal standard is a precise amount of a certain compound that is inserted into the original input sample. It is used specifically to aid in normalization of the data values, and is not part of the unknown sample being analyzed. If no internal standards are present, then all pairs of blobs which are marked as "included" by the user are used for normalization. The included flag is a feature of the GC Image software that allows the user to indicate the desire to include this blob's individual information in certain processing steps. If there are no internal standards or included blobs, then all blobs common to both images are used for normalization.

If internal standards are present, they are trusted implicitly, because they were introduced for this very purpose. However, if no internal standards are present, a small percentage of the shared blobs will sometimes be dramatically larger in one image than the other. Not only will such blobs skew the normalization factor for all blobs, but a biased normalization factor will help to hide blobs of significantly different heights which the user is likely trying to identify. This problem is solved by applying the same theory used to improve the least-squares fit transformation. Specifically, an initial scale factor is computed using all blobs in the appropriate collection. For each blob, the difference in peak height between the two images is computed. Those blobs whose difference magnitudes are in the largest 25% (rounded down to the nearest blob) are removed from further consideration, and the final normalization factor is computed using the remaining blobs. Dropping those blobs with the largest raw difference values rather than those with the largest percentage difference usually means dropping the blobs with the largest volumes and recomputing the scale using the smaller blobs. This reduces the likelihood of the scale factor being dominated by one or two enormous blobs, which would have happened in at least one series of datasets used for testing.

Chapter 3

Image-Based Comparison Methods

The focus of this research was to enhance generic image comparison techniques and develop new techniques that allow the user to more accurately and easily compare and contrast the two GC×GC datasets. The following sections detail each of the implemented comparison methods. Three well-known techniques are discussed as well as a new "fuzzy difference" comparison method and a new colorization scheme that allows more information to be conveyed than does a standard greyscale difference image. These comparison methods are illustrated using side by side thumbnails in Figure 3.7 on page 32.

3.1 Pre-existing Comparison Methods

3.1.1 Flicker

The *flicker* comparison method alternately displays each image in the same location on the screen, allowing the user to visually determine where the significant differences lie. Because the original images contain floating point pixel values with a variable range, the pixel values are scaled into an 8-bit greyscale image with pixel values in the 0–255 range for display to the screen. Darker pixels represent smaller values and lighter pixels represent larger values. Pixel values from both images are normalized using the same scale factor so that each original pixel value will map to the same display value regardless of which image is currently displayed.

A special formula is used when scaling the floating point pixel values into the 8-bit integer range for display. Because the GC×GC data typically has blobs with peak values of 100 or larger (sometimes over 10,000) next to off-peak values of less than 2, a straight linear scale would result in sharply defined peaks with little or no definition among the lower values. In order to increase the resolution at lower pixel values, the raw pixel values are shifted so that the minimum value is 1.0, then the natural logarithm of the adjusted value is computed, then this value is raised to a user-selected power (typically around 0.7). Specifically, for each power q and value v_p at pixel p,

$$v_{min} = \min_{\forall p} v_p \tag{3.1}$$

$$v'_p = (ln(v_p - v_{min} + 1))^q \tag{3.2}$$

The resulting value v'_p is then scaled linearly into the appropriate value range. The log result is raised to a power in order to increase the resolution at lower pixel values further than was possible using only the natural log. It also allows the analyst more control over the visual significance of the lower values. Equation 3.2 is used throughout the image-based comparison methods discussed here whenever floating point data must be scaled into a non-native range.

After equation 3.2 is applied to each pixel value in both images, the minimum and maximum values v'_{min} and v'_{max} at any pixel location p in either the analyzed (a) or reference (r) image are determined using

$$v'_{min} = \min_{\forall p}(\min(|a'_p|, |r'_p|)) \tag{3.3}$$

$$v'_{max} = \max_{\forall p}(\max(|a'_p|, |r'_p|)) \tag{3.4}$$

Finally, the new 8-bit value v''_p is computed as

$$v''_p = \frac{(v'_p - v'_{min})}{v'_{max}} \times 255 \tag{3.5}$$

An example flicker image is shown in Figure 3.1 on page 20.

The user may manually switch between the analyzed and reference images by clicking a button in the control window, or the software can cycle between the images automatically at a time interval specified by the user.

The flicker comparison is a useful tool for quickly comparing the shape and location of various blobs. However, the human eye's poor responsiveness to small changes in greyscale pixel intensities in areas of geographically rapid change—such as the blob peaks—makes accurate comparison of peak heights difficult.[7]

3.1.2 Addition

Another popular method for comparing images is to create what is known as an *addition image*. To do this, both the original analyzed and reference images are converted to 8-bit greyscale images using the same scale factor. The scale factor used here is the same one used for the individual flicker images detailed in Section 3.1.1 (calculated using equations 3.1 through 3.5).

A 3-band RGB image is then created by using the scaled analyzed image for the green band and the scaled reference image for the red band. Zeros are used for the

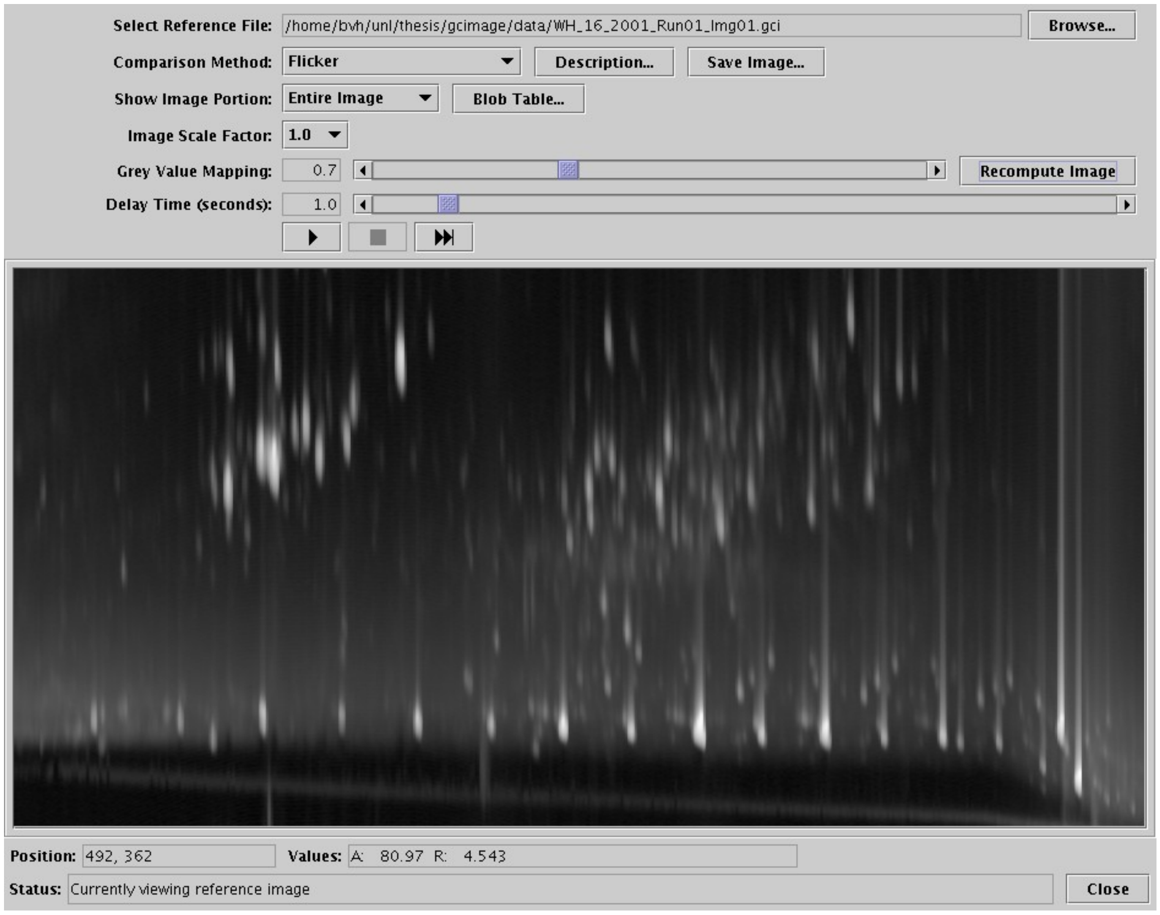

Select Reference File: /home/bvh/unl/thesis/gcimage/data/WH_16_2001_Run01_Img01.gci

Comparison Method: Flicker

Show Image Portion: Entire Image

Image Scale Factor: 1.0

Grey Value Mapping: 0.7

Delay Time (seconds): 1.0

Position: 492, 362

Values: A: 80.97 R: 4.543

Status: Currently viewing reference image

Figure 3.1: Example flicker image

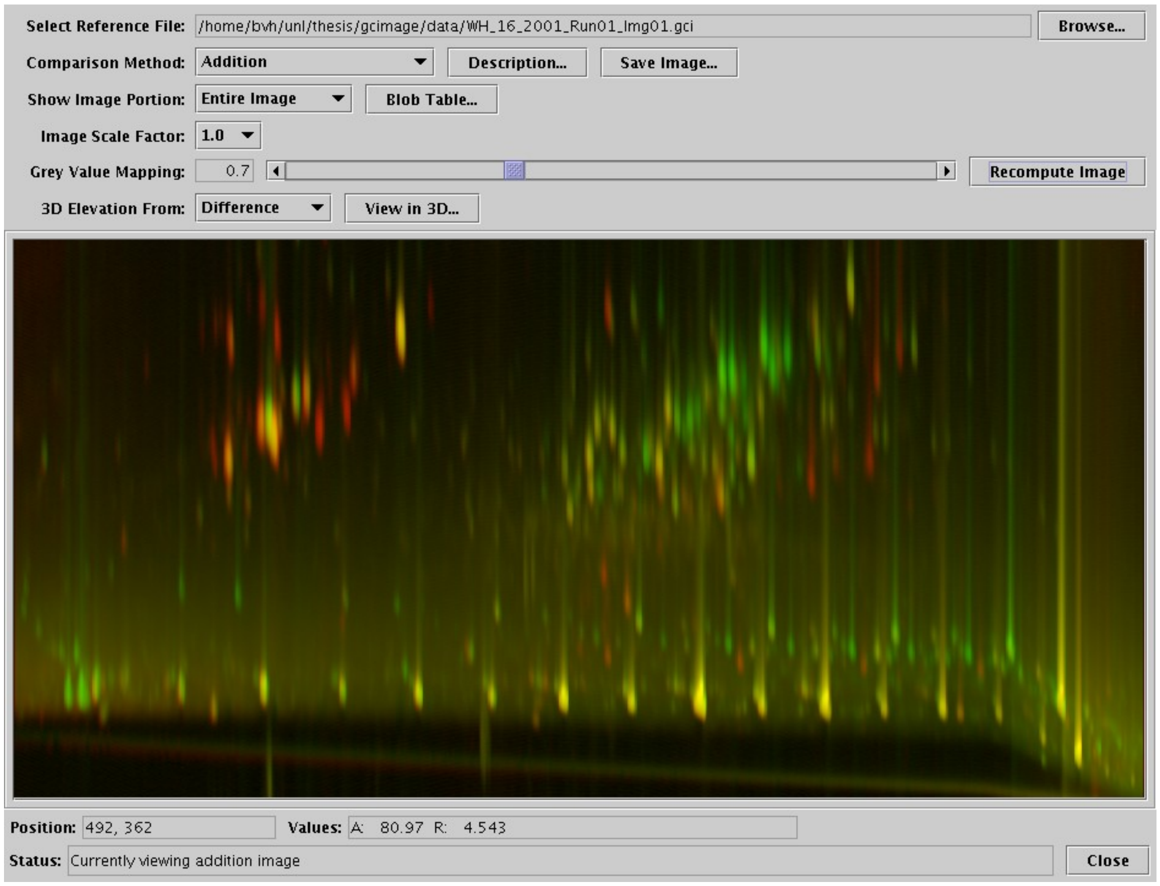
Select Reference File: /home/bvh/unl/thesis/gcimage/data/WH_16_2001_Run01_Img01.gci
Comparison Method: Addition
Show Image Portion: Entire Image
Image Scale Factor: 1.0
Grey Value Mapping: 0.7
3D Elevation From: Difference
Position: 492, 362
Values: A: 80.97 R: 4.543
Status: Currently viewing addition image

Figure 3.2: Example addition image

blue band. When this RGB image is displayed, pixels for which the analyzed image has a much larger value appear greenish, pixels for which the reference image has a much larger value appear reddish, and pixels for which both images have similar values appear yellowish. The larger the original values, the brighter the pixels. Figure 3.2 shows an example of the addition method.

The addition method allows the user to see both the differences and the original pixel magnitudes at the same time. However, in practice, it has not been as effective at illustrating smaller differences as have some of the newer methods discussed in Section 3.2. This primarily stems from the human eye's difficulty in accurately distinguishing between pure yellow and similar shades of orange or green.

3.1.3 Greyscale Difference

One of the best known and most commonly used methods of comparing two images is to subtract the individual pixel values of one image from the corresponding pixel values in the other image in order to form a *difference image* that contains only the differences between the two input images. In our GC×GC application, the reference image is subtracted from the analyzed image, so positive difference values indicate that the analyzed image had a larger value, while negative difference values indicate that the reference image was larger. At each pixel location p,

$$\Delta_p = a_p - r_p \tag{3.6}$$

where a_p is the analyzed pixel value, r_p is the reference pixel value, and Δ_p is the difference between them.

The floating point difference image is converted into an 8-bit greyscale image for display. Medium grey (display value 128) is used to represent zero difference, with positive values being brighter (display values 129 to 255) and negative values being darker (display values 1 to 127). The larger the magnitude of the difference, the closer the displayed pixel will be to white or black. The same scale factor is used for both positive and negative values, so the resulting 8-bit image will include either value 1 or 255, but perhaps not both. Pixel value 0 is reserved to indicate pixels which are outside the bounds of the reference image after it was transformed and therefore cannot be used for comparison.

Prior to scaling the difference values (Δ_p) for display, they are processed using equations 3.1 and 3.2. When used to pre-process pixel values from a difference image (including those produced by the new difference methods discussed in Section 3.2), the absolute value of v_p is used in those equations, and the sign of the original v_p

is assigned to the resulting v'_p in equation 3.2. This ensures that both positive and negative differences are scaled consistently regardless of the sign of the difference.

The value v'_p is then renamed to Δ'_p (representing the modified difference value at pixel p) and scaled linearly into the appropriate value range using the following equations. If Δ'_{max} is the maximum magnitude of any floating point value Δ'_p, the scaled display value Δ''_p is computed as

$$\Delta'_{max} = \max_{\forall p} |\Delta'_p| \tag{3.7}$$

$$\Delta''_p = \frac{\Delta'_p \times 127}{\Delta'_{max}} + 128 \tag{3.8}$$

An example difference image is shown in Figure 3.3 on page 24. Although the greyscale difference method does an adequate job of highlighting the differences between the two images, the context of those differences is lost because the magnitude of the original pixel values is not represented in the output image. In order to determine which features of the images produced the differences that are displayed, the analyst must be very familiar with the images being analyzed.

3.2 New Comparison Methods

3.2.1 Colorized Difference

In order to make the differences between the analyzed and reference images more apparent and to retain some context for those differences, the traditional greyscale difference method was modified to color code the differences and incorporate the original image pixel intensities. First, the floating point difference image is computed just as it is in the greyscale difference method (equation 3.6). For display to the

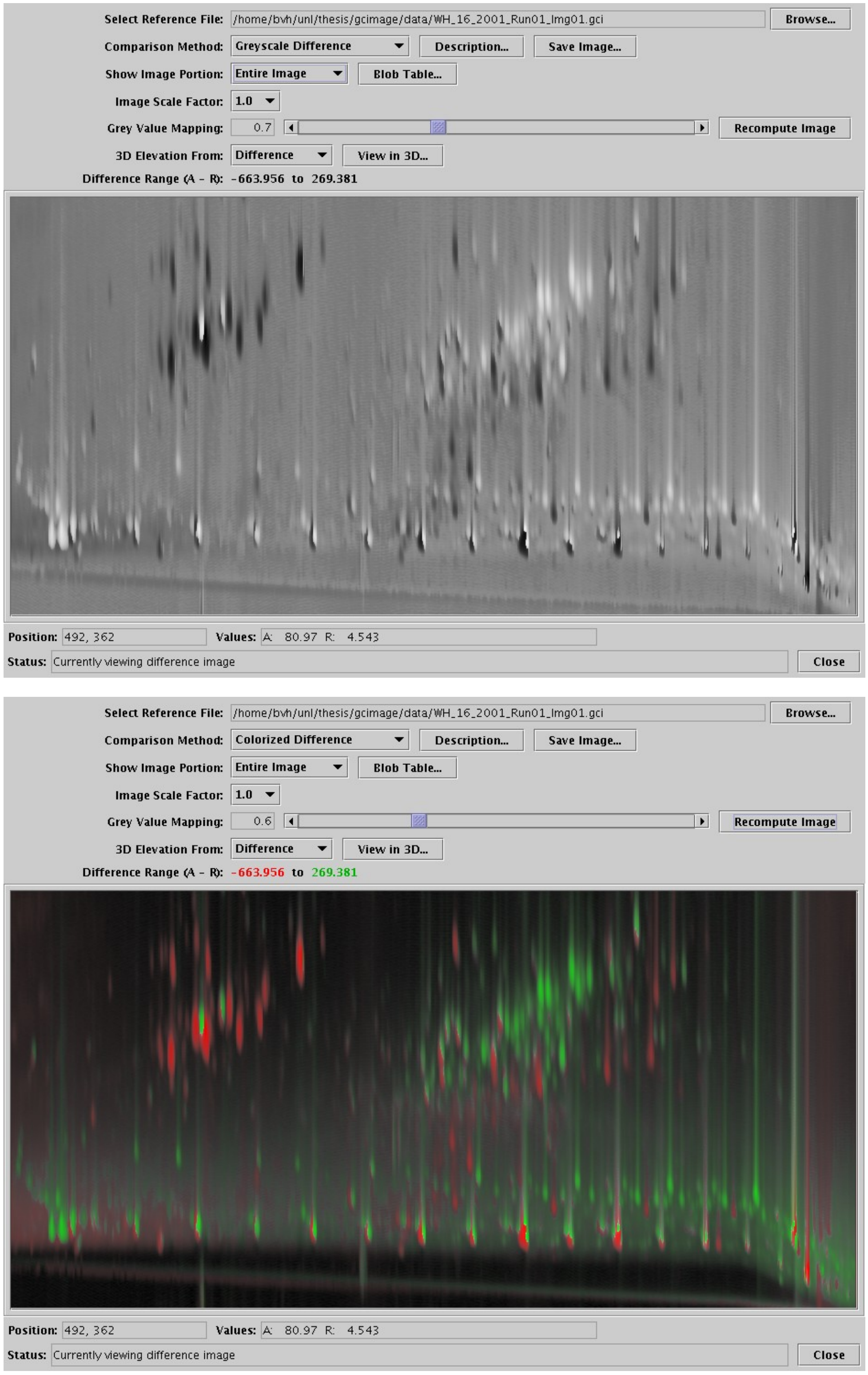

Select Reference File: /home/bvh/unl/thesis/gcimage/data/WH_16_2001_Run01_Img01.gci

Comparison Method: Greyscale Difference

Show Image Portion: Entire Image

Image Scale Factor: 1.0

Grey Value Mapping: 0.7

3D Elevation From: Difference

Difference Range (A – R): -663.956 to 269.381

Position: 492, 362 Values: A: 80.97 R: 4.543

Status: Currently viewing difference image

Select Reference File: /home/bvh/unl/thesis/gcimage/data/WH_16_2001_Run01_Img01.gci

Comparison Method: Colorized Difference

Show Image Portion: Entire Image

Image Scale Factor: 1.0

Grey Value Mapping: 0.6

3D Elevation From: Difference

Difference Range (A – R): -663.956 to 269.381

Position: 492, 362 Values: A: 80.97 R: 4.543

Status: Currently viewing difference image

Figure 3.3: Greyscale (top) and colorized (bottom) difference images

screen, the raw difference image is converted into a 24-bit RGB color image (three separate bands of 8-bit integers). The color computation is done in the Hue-Intensity-Saturation (HIS) color space.[6] The hue component of each pixel is set to pure green if the analyzed pixel value is larger or pure red if the reference pixel value is larger. The intensity component i_p of each pixel p is the maximum of the original analyzed and reference pixel values a_p and r_p, scaled to fit into the 0–1.0 range. Equation 3.2 is first applied to a_p and r_p, then

$$i_p = \frac{\max(|a'_p|, |r'_p|)}{v'_{max}} \tag{3.9}$$

using v'_{max} from equation 3.4.

The saturation component s_p is the magnitude of the raw difference value, scaled to fit into the 0–1.0 range. Equation 3.2 is first applied to each Δ_p as described in Section 3.1.3, then

$$s_p = \frac{|\Delta'_p|}{\Delta'_{max}} \tag{3.10}$$

using Δ'_{max} from equation 3.7.

After the hue, intensity, and saturation components are calculated for each pixel, they are converted to the RGB color space and stored in a 24-bit image for display to the screen.

The resulting color image shows lighter pixels where either of the original images had larger values and darker pixels where both of the original images had smaller values, thereby retaining the context for the differences that was lacking in the greyscale difference method. Pixels that had approximately equal values in both original images will appear greyish, while pixels for which there was a large difference will have bolder colors. This allows the user to see not only where the greatest differences lie between the two images, but also where those differences are located in relation to the blob peaks in the images. For comparison, the colorized and greyscale difference images are shown side by side in Figure 3.3 on page 24.

This colorization method is inspired by the work of Kunzel, who suggested using the ARgYb color space to display the original pixel values via the intensity component (A) and the differences among three radiographs via the color components (Rg and Yb).[9] Thanks to the use of the HIS color space instead of ARgYb, our algorithm is not only computationally simpler, but also allows the use of a wider range of color saturation than does Kunzel's.

3.2.2 Greyscale Fuzzy Difference

In practice, the most common difference between the analyzed and reference images comes from blob peaks that are misaligned by only a few pixels, but otherwise have very similar values. Minimizing the effect of these slightly misaligned peaks is important because they are not the differences in which the user is typically most interested. Precise alignment using piecewise or non-rigid convolution techniques is sometimes problematic with the GC$\times$GC data because most of the transformation control points (shared, named peaks) may frequently lie along a nearly straight line. A better comparison method would reduce the differences between such similar peaks while still displaying large differences for peaks that have either grown or moved significantly between the two images. The greyscale and colorized *fuzzy difference* comparison methods accomplish these goals.

To compute the fuzzy difference between the two images, the user specifies the size of a rectangular window. Typical window sizes range from 3x5 to 7x15. The difference value at each pixel in the output image is computed using a three-step process. Two intermediate difference images are first computed as follows. For each pixel location, the difference is computed between that pixel value in the analyzed image and the extents of the values found within the surrounding window from the reference image. That is, for each pixel location p, reference pixel value r_p, analyzed pixel value a_p, and difference pixel value Δ_p:

$r_{max} = \max_{p \in window} r_p$

$r_{min} = \min_{p \in window} r_p$

if $a_p < r_{min}$, then $\Delta_p = a_p - r_{min}$

else if $a_p > r_{max}$, then $\Delta_p = a_p - r_{max}$

else $\Delta_p = 0$

Note that a difference is only recognized when the analyzed pixel value is either larger or smaller than *all* of the reference pixel values in the surrounding window. This is what allows the fuzzy difference algorithm to compensate for misaligned peaks while still recognizing the actual difference in nearby peak heights.

The same intermediate difference algorithm is then repeated, with the two images swapping roles. Finally, the two intermediate difference images are combined to create the final fuzzy difference image. At each pixel location, the final image uses the pixel value from whichever intermediate difference image has the largest magnitude at that location. If the image that used the reference pixel as the center of each window is selected, its pixel value is negated in order to retain the same positive/negative relationship as the traditional difference image comparison method. The pseudocode for this algorithm is presented in Figure 3.4 on page 28. This algorithm has a computational complexity of $O(n \times m)$, where n is the number of pixels in each image and m is the number of pixels in the window.

Because blobs are typically only a few pixels wide and dozens or hundreds of pixels tall, a narrow, tall window is generally desirable. Enlarging the size of the window increases the misalignment that will be absorbed by the algorithm as well as the computation required. However, care must be taken not to make the window so large

```
function fuzzySubtract(image1, image2) {
   for (each pixel in image1) {
      minValue = PositiveInfinity;
      maxValue = NegativeInfinity;
      for (each pixel in surrounding window of image2) {
         if (image2pixel < minValue) minValue = image2pixel;
         if (image2pixel > maxValue) maxValue = image2pixel;
      }
      if (image1pixel < minValue)
         diffImagePixel = image1pixel - minValue;
      else if (image1pixel > maxValue)
         diffImagePixel = image1pixel - maxValue;
      else
         diffImagePixel = 0;
   }
   return diffImage;
}

function combineDiffs(analyzedDiff, referenceDiff) {
   for (each pixel in images) {
      if (absValue(analyzedDiffPixel) > absValue(referenceDiffPixel)
         outputImagePixel = analyzedDiffPixel;
      else
         outputImagePixel = - referenceDiffPixel;
   }
   return outputImage;
}

analyzedDiff = fuzzySubtract(analyzedImage, referenceImage);
referenceDiff = fuzzySubtract(referenceImage, analyzedImage);
fuzzyDiffImage = combineDiffs(analyzedDiff, referenceDiff);
```

Figure 3.4: Pseudocode for the fuzzy difference algorithm

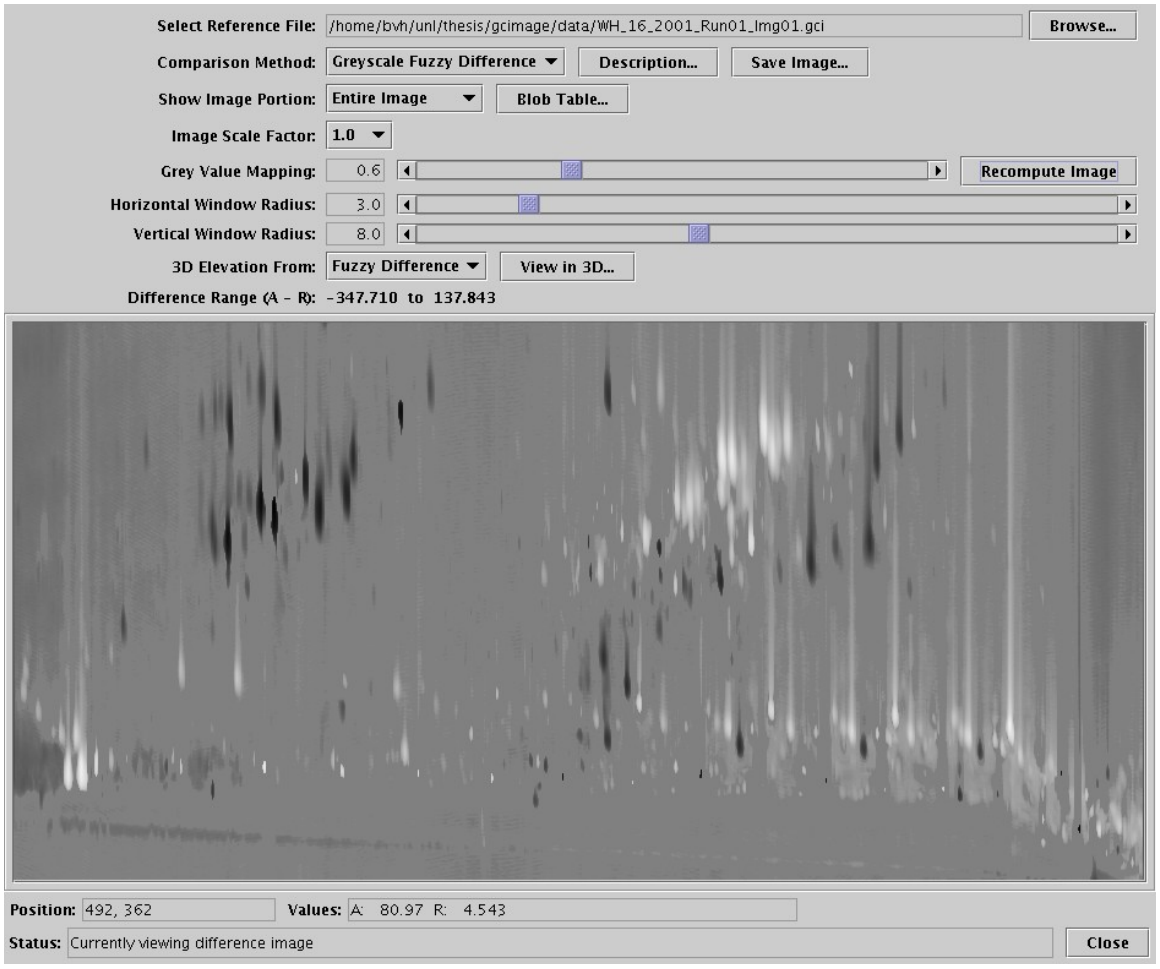
Select Reference File: /home/bvh/unl/thesis/gcimage/data/WH_16_2001_Run01_Img01.gci
Comparison Method: Greyscale Fuzzy Difference
Show Image Portion: Entire Image
Image Scale Factor: 1.0
Grey Value Mapping: 0.6
Horizontal Window Radius: 3.0
Vertical Window Radius: 8.0
3D Elevation From: Fuzzy Difference
Difference Range (A - R): -347.710 to 137.843
Position: 492, 362
Values: A: 80.97 R: 4.543
Status: Currently viewing difference image

Figure 3.5: Greyscale fuzzy difference image

that distinct, neighboring peaks are enveloped by the window and thereby hidden in the resulting image. Although the maximum usable size varies from one dataset to the next, neighboring peaks can sometimes be as close as 3 pixels from each other.

Once the fuzzy difference image is created, it is converted to an 8-bit integer image for screen display using the same method employed for the traditional greyscale difference comparison method detailed in Section 3.1.3. The resulting fuzzy difference image is shown in Figure 3.5.

Although the greyscale fuzzy difference improves on the traditional greyscale difference by removing many of the uninteresting details while retaining the interesting details, it still suffers from the same major drawback as the traditional greyscale difference—that it does not show any visible context for the resulting differences among the surrounding features of the original images.

3.2.3 Colorized Fuzzy Difference

The final comparison method takes the greyscale fuzzy difference algorithm described in Section 3.2.2 and applies the same colorization algorithm used in the colorized difference method described in Section 3.2.1, which uses intensity to indicate the pixel values from the original images and color to indicate the differences between the two images. An example of the colorized fuzzy difference image can be seen in Figure 3.6 on page 31. The resulting displayed image shares the benefits that both of those methods have over the traditional greyscale difference, namely, that it removes many uninteresting details by compensating for misaligned peaks, and that it indicates the pixel values from the original images to provide some context for the difference values. In practice, the colorized fuzzy difference algorithm appears to effectively highlight the interesting differences in blob peak heights and shapes, even when peaks are slightly misaligned.

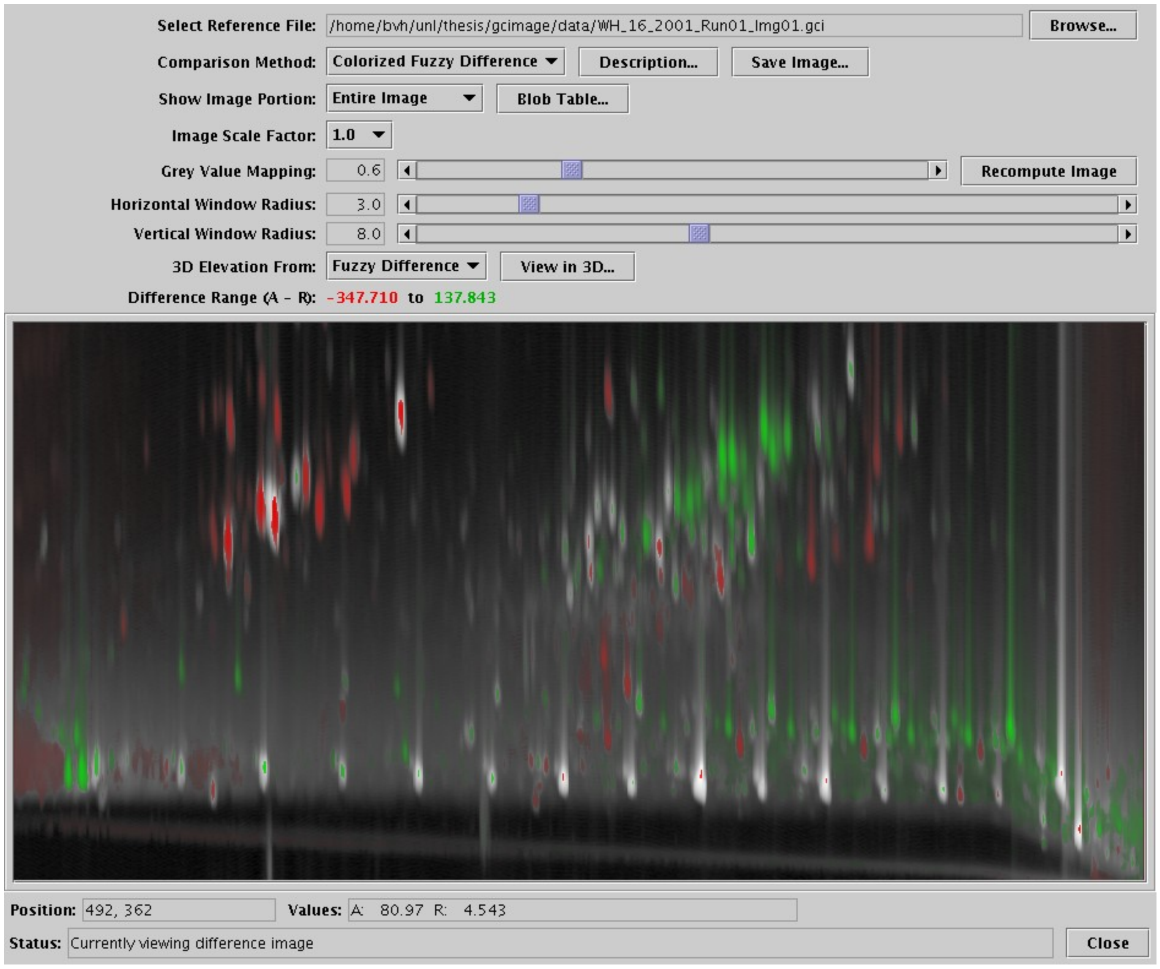
Select Reference File: /home/bvh/unl/thesis/gcimage/data/WH_16_2001_Run01_Img01.gci

Comparison Method: Colorized Fuzzy Difference

Show Image Portion: Entire Image

Image Scale Factor: 1.0

Grey Value Mapping: 0.6

Horizontal Window Radius: 3.0

Vertical Window Radius: 8.0

3D Elevation From: Fuzzy Difference

Difference Range (A - R): -347.710 to 137.843

Position: 492, 362

Values: A: 80.97 R: 4.543

Status: Currently viewing difference image

Figure 3.6: Colorized fuzzy difference image

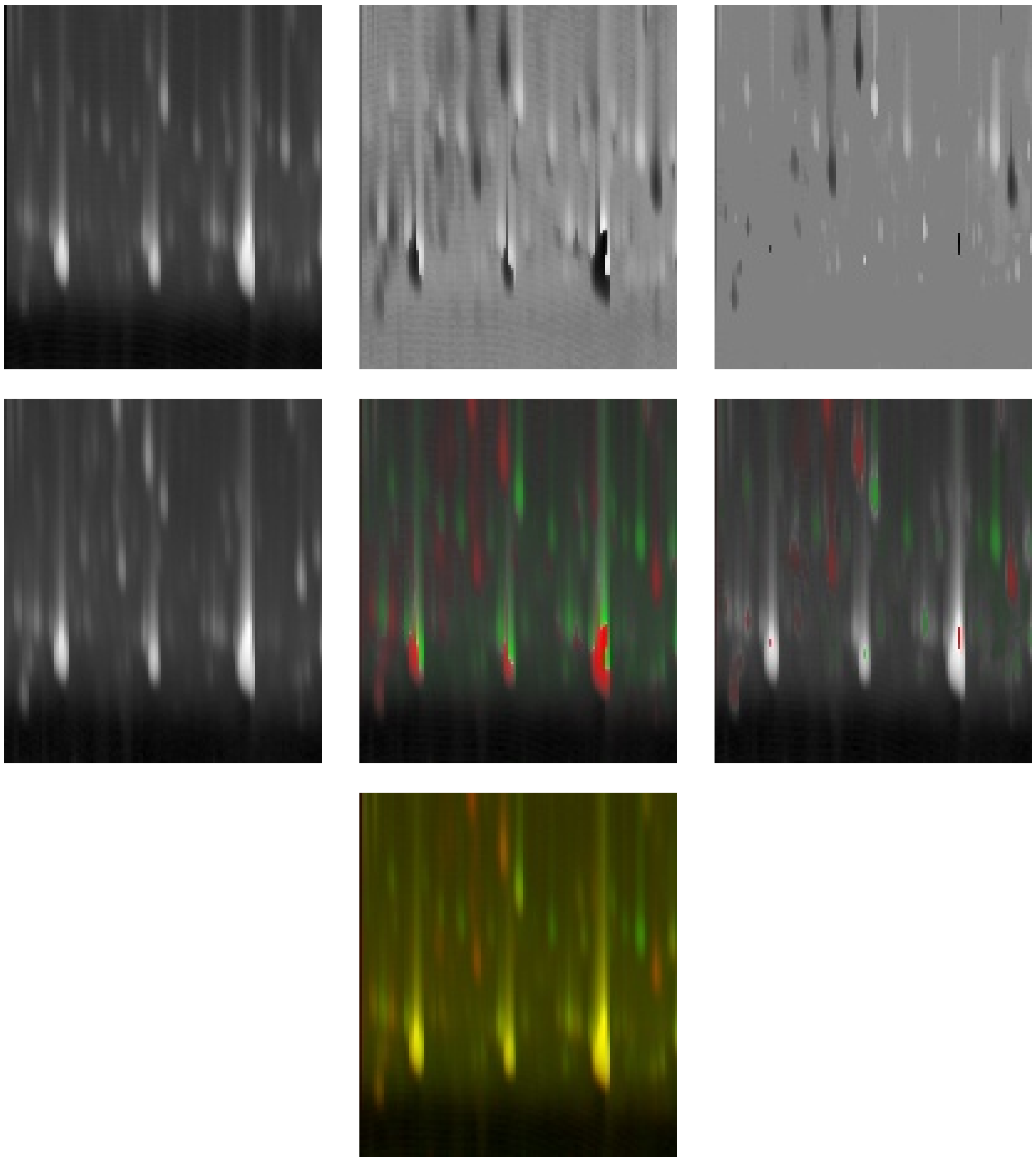

Figure 3.7: Comparison image thumbnails. Top row: original analyzed image (left), greyscale difference (center), and greyscale fuzzy difference (right). Middle row: original reference image (left), colorized difference (center), and colorized fuzzy difference (right). Bottom row: addition.

Chapter 4

Additional Dataset Analysis

Once the displayable images have been generated for any of the image-based comparison methods, additional operations can be performed on the datasets to enhance the user's understanding of the data.

4.1 Masking Images

Although the comparison process attempts to remove uninteresting differences and highlight interesting ones, the users may want to mask off certain areas of an image so that comparisons are only displayed for a particular subsection of the image area. To accomplish this, the image comparison procedure allows the user to mask off a variety of different areas described in Table 4.1 on page 35. This mask is applied as the final step after all other preprocessing and comparison image computation has been performed on the entire image area. Pixels outside the mask's active area are displayed as a null value appropriate for the currently selected comparison method. For example, the addition method would use black, while the greyscale difference method would use medium grey. Examples of masked and unmasked difference images are shown in Figure 4.1 on page 34.

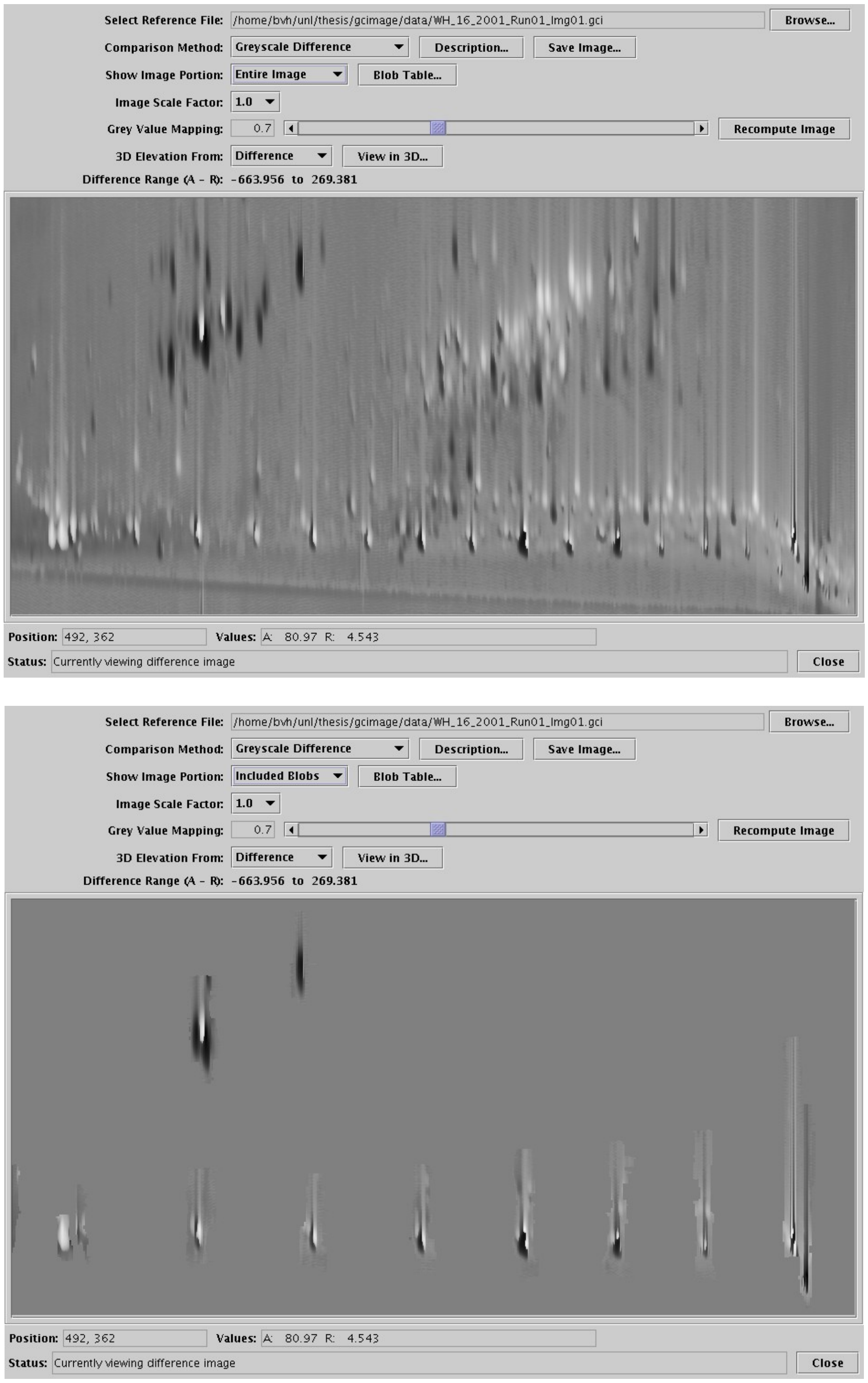

Select Reference File: /home/bvh/unl/thesis/gcimage/data/WH_16_2001_Run01_Img01.gci
Comparison Method: Greyscale Difference
Show Image Portion: Entire Image
Image Scale Factor: 1.0
Grey Value Mapping: 0.7
3D Elevation From: Difference
Difference Range (A - R): -663.956 to 269.381
Position: 492, 362 Values: A: 80.97 R: 4.543
Status: Currently viewing difference image

Select Reference File: /home/bvh/unl/thesis/gcimage/data/WH_16_2001_Run01_Img01.gci
Comparison Method: Greyscale Difference
Show Image Portion: Included Blobs
Image Scale Factor: 1.0
Grey Value Mapping: 0.7
3D Elevation From: Difference
Difference Range (A - R): -663.956 to 269.381
Position: 492, 362 Values: A: 80.97 R: 4.543
Status: Currently viewing difference image

Figure 4.1: Entire greyscale difference image (top) and the same image with a mask showing only included blobs (bottom)

Mask Type	Active Area Displayed
Entire Image	The entire image
All Blobs	The area covered by all blobs in either image
Included Blobs	The area covered by blobs in either image which the user has designed as "included"
Selected Blobs	The area covered by blobs in either image which the user has interactively selected
Included Shapes	The area covered by shapes marked as "included," minus any shapes marked as "excluded"

Table 4.1: Available image mask selections

4.2 Tabular Data

In addition to the image-based comparison methods outlined in Chapter 3, the numerical characteristics of the blobs defined in each GC×GC dataset may be compared side by side in a blob comparison table. The only blobs displayed in the table are those which have the same compound name as exactly one blob in the other image.

The features displayed for each blob are listed in Table 4.2 on page 36. For each feature, the values for the analyzed and reference image are listed side by side in the table. For those features marked in Table 4.2 with an asterisk (*), the difference between the feature values of the two images is also listed. To aid in analysis, the table rows containing the blobs may be ordered using any feature for either image or any feature difference between the images by clicking the mouse on the header of the appropriate column. The contents of this table may be saved to a comma-separated, quoted, ASCII text file for later importation into a variety of spreadsheet or database applications.

If one or more blobs in the table are selected by clicking the appropriate rows with the mouse, those rows are highlighted and the outlines of those blobs are drawn on top of the current comparison image in the image comparison window. The analyzed blob is outlined in green and the reference blob is outlined in red. This allows the

Feature	Description
ID Number	Unique identifier for each blob within each dataset
Group Name	Name of the group to which this blob belongs
Inclusion Status	Whether or not the blob is marked for inclusion
Internal Standard	ID number for the associated internal standard blob
Peak Location	Pixel coordinates of the peak value along each axis *
Peak Value	The highest pixel value in the blob *
Area	The number of pixels encompassed by the blob *
Volume	The sum of all pixel values encompassed by the blob *

Table 4.2: Blob features displayed in the tabular comparison

user to easily locate the blobs of interest; for example, the corresponding blobs with the largest volume difference. The blob comparison table and a greyscale difference image with several blobs outlined are shown in Figures 4.2 and 4.3 on page 37.

4.3 Three-Dimensional Visualization

Although the various image-based comparison methods combined with the tabular data help the user interpret the datasets, it is sometimes helpful to visualize the GC$\times$GC image data as an elevation map, with blob peaks and background pixels emulating mountains and valleys. The software allows the user to view the image data in an interactive, three-dimensional environment. Pixels from one of several image sources are treated as an elevation map, and the image generated by the currently selected comparison method is draped over the surface of the elevation map to provide coloration. The user can then view the data from various distances or viewing angles and can locate the viewer's position anywhere in or around the data.

This capability is available for single images in the GC Image package, and was modified in order to enhance the visualization capabilities of the image comparison package. If any areas of the comparison image have been masked out or any blob outlines have been drawn into this image, those changes are transfered into the 3D

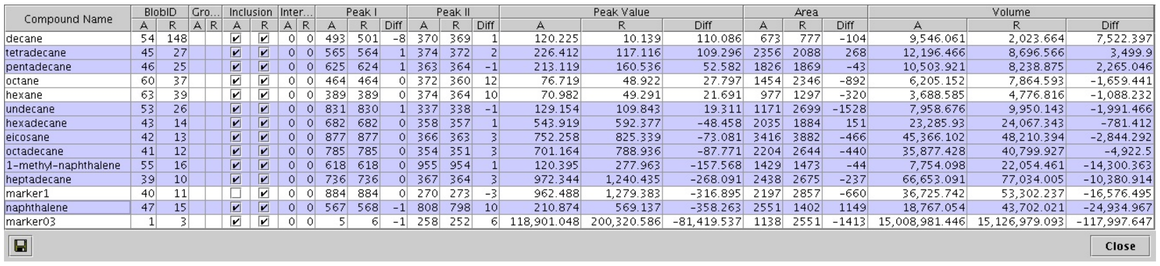

Compound Name	BlobID		Gro...		Inclusion		Inter...		Peak I			Peak II			Peak Value			Area			Volume		
	A	R	A	R	A	R	A	R	A	R	Diff	A	R	Diff	A	R	Diff	A	R	Diff	A	R	Diff
decane	54	148			✓	✓	0	0	493	501	-8	370	369	1	120.225	10.139	110.086	673	777	-104	9,546.061	2,023.664	7,522.397
tetradecane	45	27			✓	✓	0	0	565	564	1	374	372	2	226.412	117.116	109.296	2356	2088	268	12,196.466	8,696.566	3,499.9
pentadecane	46	25			✓	✓	0	0	625	624	1	363	364	-1	213.119	160.536	52.582	1826	1869	-43	10,503.921	8,238.875	2,265.046
octane	60	37			✓	✓	0	0	464	464	0	372	360	12	76.719	48.922	27.797	1454	2346	-892	6,205.152	7,864.593	-1,659.441
hexane	63	39			✓	✓	0	0	389	389	0	374	364	10	70.982	49.291	21.691	977	1297	-320	3,688.585	4,776.816	-1,088.232
undecane	53	26			✓	✓	0	0	831	830	1	337	338	-1	129.154	109.843	19.311	1171	2699	-1528	7,958.676	9,950.143	-1,991.466
hexadecane	43	14			✓	✓	0	0	682	682	0	358	357	1	543.919	592.377	-48.458	2035	1884	151	23,285.93	24,067.343	-781.412
eicosane	42	13			✓	✓	0	0	877	877	0	366	363	3	752.258	825.339	-73.081	3416	3882	-466	45,366.102	48,210.394	-2,844.292
octadecane	41	12			✓	✓	0	0	785	785	0	354	351	3	701.164	788.936	-87.771	2204	2644	-440	35,877.428	40,799.927	-4,922.5
1-methyl-naphthalene	55	16			✓	✓	0	0	618	618	0	955	954	1	120.395	277.963	-157.568	1429	1473	-44	7,754.098	22,054.461	-14,300.363
heptadecane	39	10			✓	✓	0	0	736	736	0	367	364	3	972.344	1,240.435	-268.091	2438	2675	-237	66,653.091	77,034.005	-10,380.914
marker1	40	11			☐	✓	0	0	884	884	0	270	273	-3	962.488	1,279.383	-316.895	2197	2857	-660	36,725.742	53,302.237	-16,576.495
naphthalene	47	15			✓	✓	0	0	567	568	-1	808	798	10	210.874	569.137	-358.263	2551	1402	1149	18,767.054	43,702.021	-24,934.967
marker03	1	3			✓	✓	0	0	5	6	-1	258	252	6	118,901.048	200,320.586	-81,419.537	1138	2551	-1413	15,008,981.446	15,126,979.093	-117,997.647

Figure 4.2: Blob comparison table with nine blobs selected

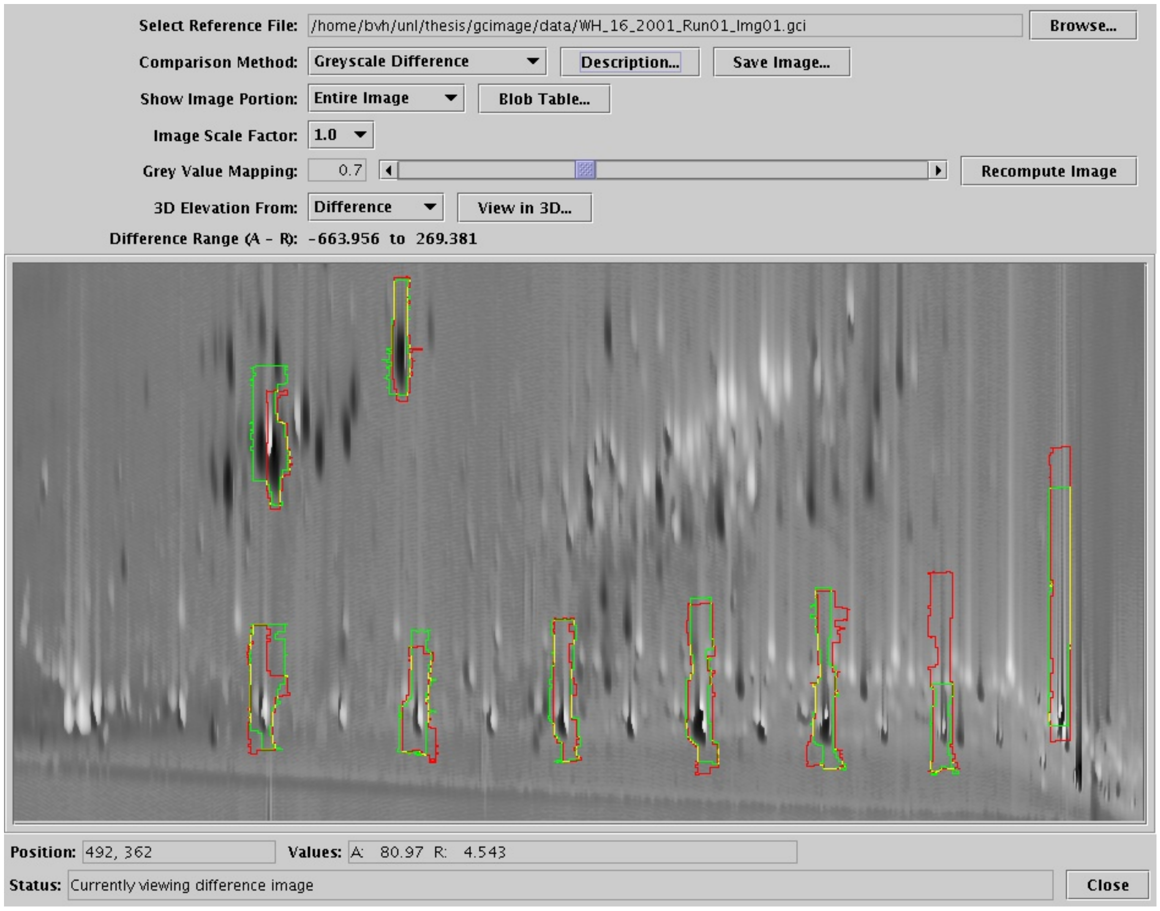

Select Reference File: /home/bvh/unl/thesis/gcimage/data/WH_16_2001_Run01_Img01.gci

Comparison Method: Greyscale Difference

Show Image Portion: Entire Image

Image Scale Factor: 1.0

Grey Value Mapping: 0.7

3D Elevation From: Difference

Difference Range (A – R): -663.956 to 269.381

Position: 492, 362

Values: A: 80.97 R: 4.543

Status: Currently viewing difference image

Figure 4.3: Greyscale difference image with blob outlines overlaid

view as well.

For the elevation map, the user may select one of four different images:

- The original analyzed image data.
- The original reference image data (after transformation and normalization).
- An image containing the maximum pixel value at each location from either the analyzed or reference image.
- The difference image. If either of the fuzzy difference comparison methods is selected, the fuzzy difference is used. For all other comparison methods, the traditional difference is used.

Masked areas, if selected, are applied to the elevation map as well, with inactive pixels having a value of zero. The ability to drape any of the comparison images over a variety of different elevation maps allows the user great versatility in analyzing the data. It also allows even the greyscale difference comparisons (traditional or fuzzy) to be viewed in the context of the original pixel data—something that is not possible using only a two-dimensional image. Another advantage of the 3D view is the user's ability to compare elevation peak heights by viewing the image from the side and sighting across the tops of the elevation peaks. Sample 3D views are shown in Figure 4.4 on page 39.

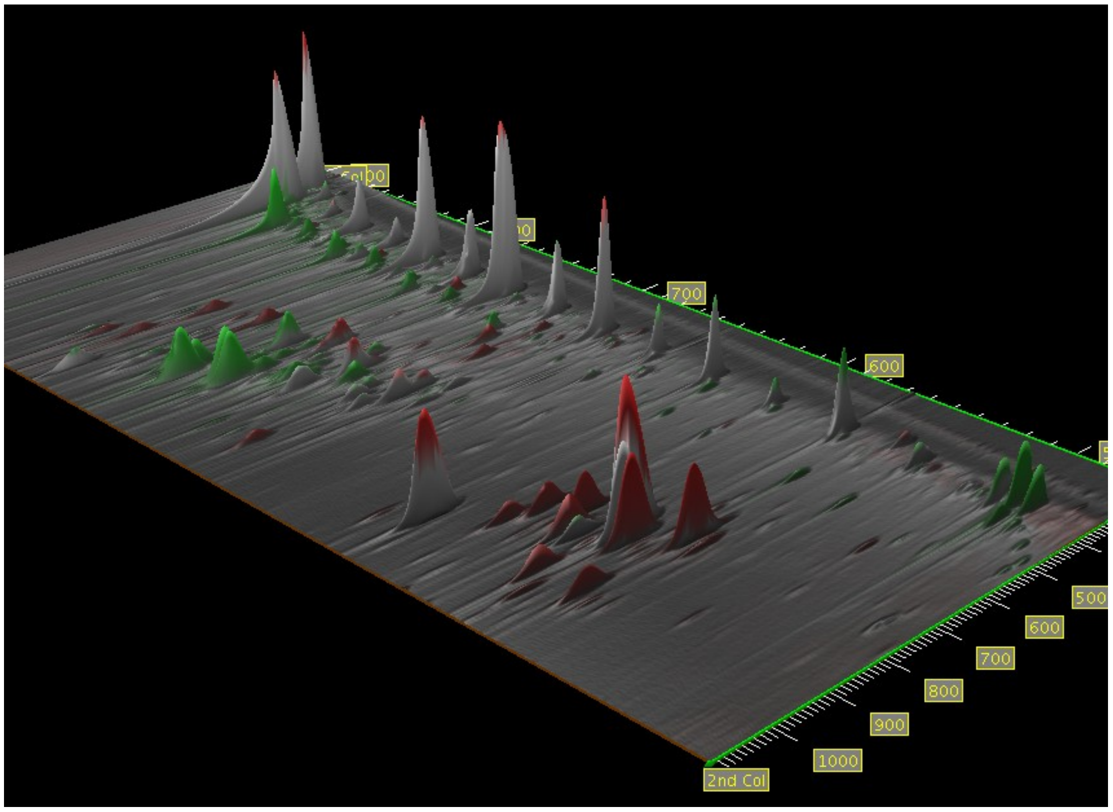

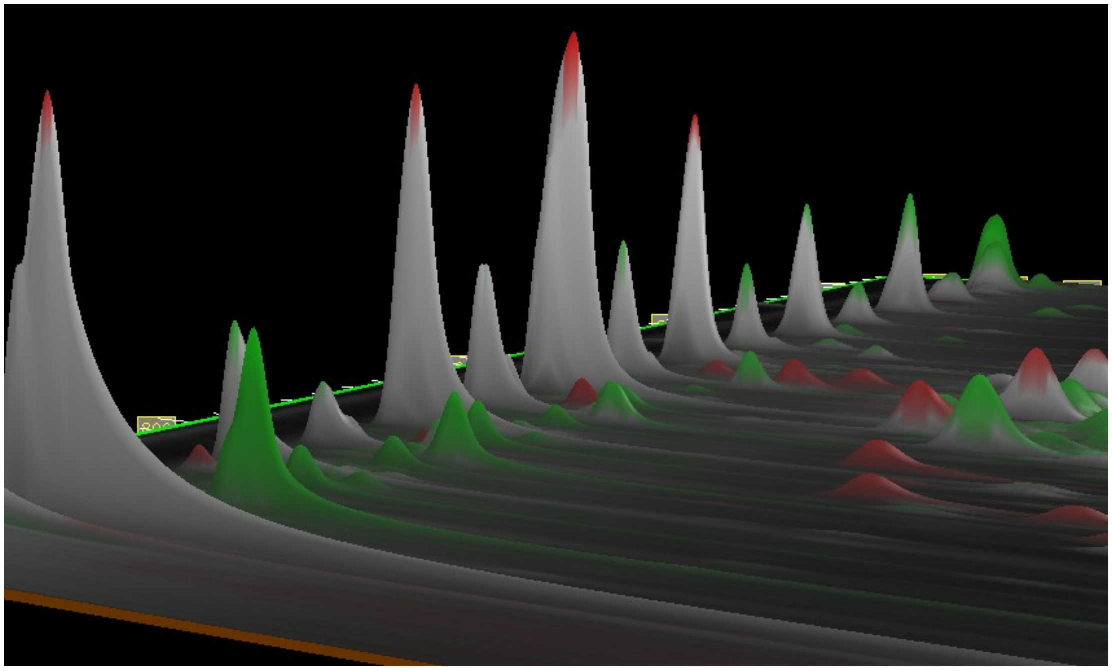

Figure 4.4: 3D renderings of the colorized fuzzy difference image draped over the maximum value elevation map

Chapter 5

Conclusions and Future Work

Initial reports from GC×GC analysts with the United States Coast Guard Academy are promising. The registration and normalization methods detailed in Chapter 2 for matching peak locations and other features of the reference image to the analyzed image are adequate for most analyses. However, there is still room for future work with the selection of control points or alternate registration algorithms to improve this process. Improvements in image registration could reduce the uninteresting differences generated by the various comparison methods and therefore reduce, but probably not eliminate, the need for the fuzzy difference algorithms presented in Sections 3.2.2 and 3.2.3.

The fuzzy difference comparison methods do an excellent job of eliminating most of the artifacts resulting from the mis-alignment of features between images. However, enhancements to this algorithm may still be possible. The proper selection of the window size is critical to the algorithm's ability to merge corresponding features between the two images while still indicating differences for nearby, unrelated features. Automated selection of the window size—perhaps using information gleaned from the registration process on the amount of mis-alignment of corresponding peak locations—

could be a valuable tool for analysts.

The ability to locate the largest differences between two datasets has also proven to be a valuable asset to analysts. Variations of this capability are provided by both the tabular view from Section 4.2 and the three-dimensional view from Section 4.3.

Although determining the differences between two images is important, determining the location of those differences relative to the blob peaks and other features within the original images is also critical for analysts. The greyscale difference algorithms provided by many image analysis software packages lack this capability. The colorized difference algorithms from Sections 3.2.1 and 3.2.3 have solved this problem by using hue to indicate differences and brightness to indicate the original pixel values. The ability within the three-dimensional view to overlay any of the comparison images on a variety of elevation maps further improves an analyst's ability to visualize how the differences correspond to the original feature locations.

It has been suggested that the use of red and green as the primary colors for the addition (Section 3.1.2) and colorized difference algorithms may prove problematic for analysts who are red-green color blind. Although these colors seem to work well for most users, further work could be done to choose more universally distinguishable colors or perhaps to allow the analyst to configure which colors are used by the software.

In addition to improving the data-based comparison techniques discussed here, the area of model-based comparisons of features such as peak shape and other statistics has many opportunities for future research. The use of such features as control points for image registration may provide a significant improvement in accuracy over the peak locations current employed.

While the work discussed here was performed on comprehensive two-dimensional gas chromatography data, these techniques could easily be applied to other two-dimensional chromatography processes such as LC×LC (liquid chromatography) or two-dimensional gel electrophoresis.

Finally, the image-based comparison methods discussed here in Chapter 3 could be extended to handle the three-dimensional data generated by GC^3 (comprehensive 3D gas chromatography) as outlined by Ledford.[5] The computation of the comparison data would be straightforward. Screen display of such data would likely use an interactive 3D environment similar to what is currently used for 3D mapping of 2D data described in Section 4.3. Rather than draping a color image over an elevation map, this data would likely be comprised of a 3D rectangle of "voxels" (volumetric pixels). The proper selection of color and transparency for each voxel's data value would be critical to the interpretation of such data. Ledford suggests that the number of voxels created by the GC^3 process should be similar to the number of pixels currently generated by GC×GC, although if that number increases significantly, memory usage and CPU time may be a concern.

Appendix A

Programming Environment

These comparative visualization techniques were implemented as a part of the *GC Image* software package published by GC Image, LLC, and marketed Zoex Corporation. *GC Image* is a large software package for use in the analysis of datasets resulting from comprehensive two-dimensional gas chromatography (GC$\times$GC). It is written in the Java programming language using J2SE version 1.4.2, Java3D version 1.3.1, and JAI version 1.1.2. Development was done simultaneously on Debian GNU/Linux, Macintosh OS/X, and Windows XP.

Bibliography

[1] Howard Anton. *Elementary Linear Algebra*. John Wiley & Sons Ltd, fifth edition, 1987.

[2] Wolfgang Bertsch. Two-dimensional gas chromatography. concepts, instrumentation, and applications—Part 2: Comprehensive two-dimensional gas chromatography. *Journal of High Resolution Chromatography*, 23(3):167–181, March 2000.

[3] Jan Blomberg. *Multidimensional GC-based separations for the oil and petrochemical industry*. PhD thesis, Vrije Universiteit Amsterdam, 2002.

[4] Richard L. Burden and J. Douglas Faires. *Numerical Analysis*. PWS-KENT Publishing Company, fourth edition, 1989.

[5] Edward B. Ledford, Jr. and Chris A. Billesbach. GC^3: Comprehensive three-dimensional gas chromatography. *Journal of High Resolution Chromatography*, 23(3):205–207, March 2000.

[6] James D. Foley, Andries van Dam, Steven K. Feiner, and John F. Hughes. *Computer Graphics: Principles and Practice*. Addison-Wesley Publishing Company, Inc., second edition, 1990.

[7] Rafael C. Gonzalez and Richard E. Woods. *Digital Image Processing*. Addison-Wesley Publishing Company, Inc., 1992.

[8] James Harynuk, Tadeusz Gorecki, and Colin Campbell. On the interpretation of GCxGC data. *LC-GC North America*, 20(9):876–887, September 2002.

[9] A. Kunzel. Controlled color coding in digital subtraction radiography. *CARS'99 Computer Assisted Radiology and Surgery. Proceedings of the 13th International Congress and Exhibition*, pages 922–926, June 1999.

[10] P. Lemkin, L. Lipkin, B. Shapiro, M. Wade, M. Schultz, E. Smith, C. Merril, M. van Keuren, and W. Oertel. Software aids for the analysis of 2D gel electrophoresis images. *Computers and Biomedical Research*, 12(6):517–44, December 1979.

[11] Z. Liu and J.B. Phillips. Comprehensive two-dimensional gas chromatography using an on-column thermal modulator interface. *Journal of Chromatographic Science*, 29:227–231, June 1991.

[12] Luigi Mondello, Alastair C. Lewis, and Keith D. Bartle. *Multidimensional Chromatography.* John Wiley & Sons Ltd, 2002.

[13] Morton Nadler and Eric P. Smith. *Pattern Recognition Engineering.* John Wiley & Sons Ltd, 1993.

[14] M. Ni and S.E. Reichenbach. A statistics-guided progressive RAST algorithm for peak template matching in GCxGC. *Proceedings of the 2003 IEEE Workshop on Statistical Signal Processing*, pages 383–386, 2003.

[15] J.B. Phillips and J. Beens. Comprehensive two-dimensional gas chromatography: a hyphenated method with strong coupling between the two dimensions. *Journal of Chromatography A*, 856(1–2):331–347, September 1999.

[16] S.E. Reichenbach, M. Ni, V. Kottapalli, and A. Visvanathan. Information technologies for comprehensive two-dimensional gas chromatography. *Chemometrics and Intelligent Laboratory Systems*, 71(2):107–120, 2004.

[17] Azriel Rosenfeld and Avinash C. Kak. *Digital Picture Processing*, volume 2. Academic Press, Inc., second edition, 1982.

[18] Q. Shen, A. Pang, and S. Uselton. Data level comparison of wind tunnel and computational fluid data dynamics data. *Proc. IEEE Visualization 1998*, pages 415–418, October 1998.

[19] X.-Q. Shi, I. Eklund, G. Tronje, U. Welander, H.C. Stamatakis, P.-E. Engstrom, and G. Norhagen Engstrom. Comparison of observer reliability in assessing alveolar bone changes from color-coded with subtraction radiographs. *Dentomaxillofacial Radiology*, 28:31–36, 1999.

[20] Q. Song, A. Savant, S.E. Reichenbach, and E.B. Ledford. Digital image processing for a new type of chemical separation system. *Proceedings of the SPIE - The International Society for Optical Engineering*, 3808:2–11, 1999.